Icarus 317 (2019) 470–478

Contents lists available at ScienceDirect

Icarus

journal homepage: www.elsevier.com/locate/icarus

Mars global simulant MGS-1: A Rocknest-based open standard for basaltic martian regolith simulants

Kevin M. Cannon[a,*], Daniel T. Britt[a], Trent M. Smith[b], Ralph F. Fritsche[b], Daniel Batcheldor[c]

[a] Department of Physics, University of Central Florida, 4111 Libra Drive, Physical Sciences Building 430, Orlando, FL 32816, USA
[b] NASA Kennedy Space Center, Titusville, FL 32899, USA
[c] Florida Institute of Technology, Melbourne, FL 32901, USA

A B S T R A C T

The composition and physical properties of martian regolith are dramatically better understood compared to just a decade ago, particularly through the use of X-ray diffraction by the Curiosity rover. Because there are no samples of this regolith on Earth, researchers and engineers rely on terrestrial simulants to test future hardware and address fundamental science and engineering questions. Even with eventual sample return, the amount of material brought back would not be enough for bulk studies. Many existing Mars simulants were designed 10 or 20 years ago based on a more rudimentary understanding of martian surface materials. Here, we describe the Mars Global Simulant (MGS-1), a new open standard designed as a high fidelity mineralogical analog to global basaltic regolith on Mars, as represented by the Rocknest windblown deposit at Gale crater. We developed prototype simulants using the MGS-1 standard and characterized their basic physical properties, bulk chemistry, spectral properties, and volatile content. The MGS-1 based simulant compares favorably to rover and remote sensing observations from Mars, and offers dramatic improvements over past simulants in many areas. Modest amounts of simulant will be produced by the Center for Lunar & Asteroid Surface Science (CLASS) Exolith Lab to distribute to other researchers. By publishing the mineral recipe and production methods, we anticipate that other groups can re-create the simulant and modify it as they see fit, leading to a more sustainable model for simulant production and the possibility of extending the simulant for different regions on Mars or for different applications.

1. Introduction

Planetary materials available for laboratory study come from a handful of sample return missions, as well as a large meteorite collection dominated by ordinary chondrites. Because actual planetary samples tend to be rare and often expensive, various groups have produced synthetic planetary materials, or “simulants”, that aim to replicate one or more features of a reference sample. These features commonly include the geomechanical and compositional characteristics of rocks, regolith or fine dust. Simulants have been used to test engineering hardware (e.g., Bernold, 1991), for astrobiology studies (e.g., de Vera et al., 2004), and plant growth experiments (e.g., Wamelink et al., 2014), among other applications. However, past simulants (particularly lunar ones) have been plagued by a lack of quality control (Taylor et al., 2016). Previous simulants often sacrificed accuracy for convenience, had poor documentation, and the resulting products have been assumed to be appropriate for all types of research. Perhaps more problematic is that simulants have usually been produced in large batches, and when the initial batch runs out it can be difficult to re-create the original material.

Simulants for martian regolith (informally, soil) are prone to these same issues, and the most cited martian simulants are no longer publically available. The most prominent Mars simulant is Johnson Space Center JSC Mars-1 (Allen et al., 1998), which was later reproduced as JSC Mars-1A by Orbitec when the original supply ran out. However, the Orbitec simulant website was taken down sometime in 2017 and it appears that JSC Mars-1 and Mars-1A are no longer available outside of NASA. The other notable Mars simulant is Mojave Mars Simulant (MMS) (Peters et al., 2008), that is also unavailable outside of NASA. An education company called The Martian Garden sells two simulants that are reported to be derived from the same source material as MMS, but in fact they have mined a highly altered red cinder material instead of the original Saddleback Basalt (see below). The utility of these simulants (JSC Mars-1, MMS, and their updated versions) comes mostly from the fact that they are granular, roughly basaltic composition materials: this may be appropriate for certain uses, but inappropriate for others.

The goal of this work is to develop an open standard for a martian regolith simulant (Mars Global Simulant, MGS-1) with high fidelity in mineral, chemical, volatile, and spectral properties compared to an appropriate reference material, in this case the windblown soil Rocknest at Gale crater (Fig. 1(a)) (Bish et al., 2013; Blake et al., 2013; Leshin et al., 2013; Minitti et al., 2013; Archer et al., 2014; Sutter et al., 2017; Achilles et al., 2017). We produced and analyzed prototype

* Corresponding author.
E-mail address: cannon@ucf.edu (K.M. Cannon).

https://doi.org/10.1016/j.icarus.2018.08.019
Received 30 April 2018; Received in revised form 24 July 2018; Accepted 21 August 2018
Available online 24 August 2018
0019-1035/

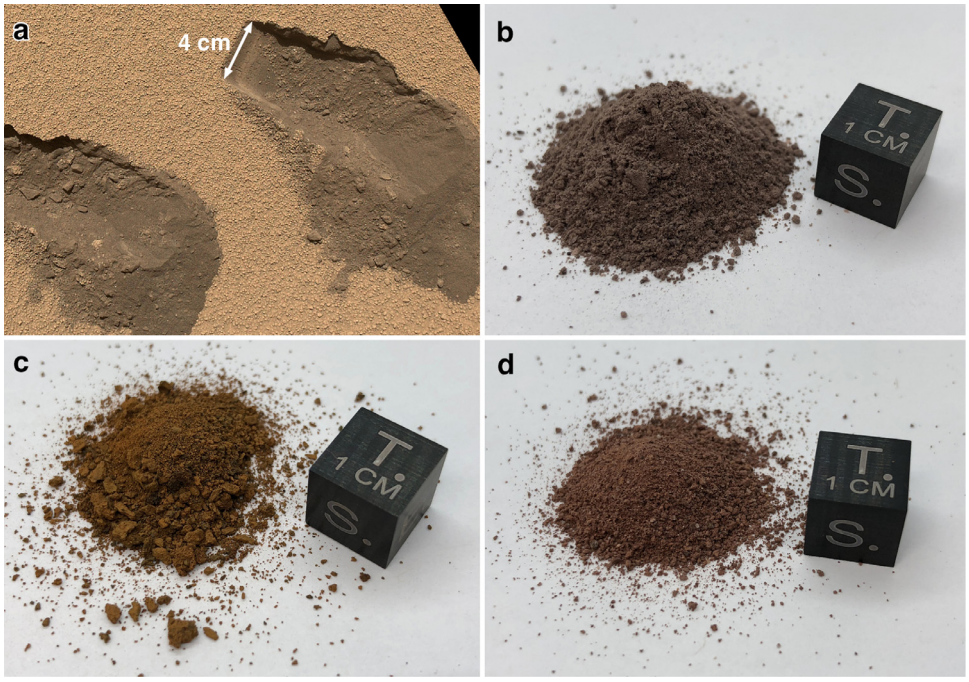

Fig. 1. Comparison of martian simulants. (a) MAHLI image of the scooped Rocknest soil; image credit NASA/JPL-Caltech/MSSS. (b) Photograph of MGS-1 prototype simulant produced for this work. (c) Photograph of JSC Mars-1. (d) Photograph of MMS-1 sold by the Martian Garden company.

simulants (Fig. 1(b)) using this standard, some of which are already being used in ongoing soil remediation and plant growth studies, and for testing curation protocols for future Mars sample return. The CLASS Exolith Lab is building the capacity to produce modest quantities of MGS-1 based simulant and make it available to the community. However, as an open standard the same mineral recipe and methods described below can be used to re-produce MGS-1 and modify it as desired (Section 5.2).

1.1. Previous Mars simulants

JSC Mars-1 and MMS have been used in a variety of laboratory studies as "soil simulants" (e.g., Shkuratov et al., 2002; de Vera et al., 2004; Arvidson et al., 2009; Zacny et al., 2013), but these simulants are based on early studies of martian regolith. JSC Mars-1 (Fig. 1(c)) was sourced from an altered palagonitic tephra at the Pu'u Nene cinder cone between Mauna Loa and Mauna Kea in Hawaii (Allen et al., 1998). It consists mostly of X-ray amorphous palagonite (a gel-like hydrated and oxidized alteration product of volcanic glass; Stroncik and Schmincke (2002)), with crystallites of plagioclase and magnetite. JSC Mars-1 was designed as a spectral simulant, in that the nanophase iron oxides (npOx) present in the tephra produced a good match to the visible/near-infrared (VNIR) spectra from dusty deposits on Mars, particularly at shorter wavelengths (Evans and Adams, 1979; Bell et al., 1993; Morris et al., 1993, 2001; Allen et al., 1998).

MMS was designed as a geotechnical simulant and was sourced from the Saddleback Basalt near the NASA Jet Propulsion Laboratory: it consists of crystalline plagioclase, pyroxene, magnetite, and hematite, with trace ilmenite and olivine (Peters et al., 2008). Although the original MMS is not available outside of NASA, The Martian Garden company sells a product marketed as Mojave Mars Simulant, renamed MMS-1 (Fig. 1(d)), and an "enhanced" version, MMS-2. MMS-2 is described as being spiked with iron oxide, magnesium oxide, and unnamed sulfates and silicates. However, The Martian Garden company had no contact with the creators of MMS, and their simulants do not resemble the original version (compare Fig. 1(d) with Fig. 2 in Peters et al. (2008)). The company is instead mining the highly altered red cinder material described by Beegle et al. (2007) instead of the

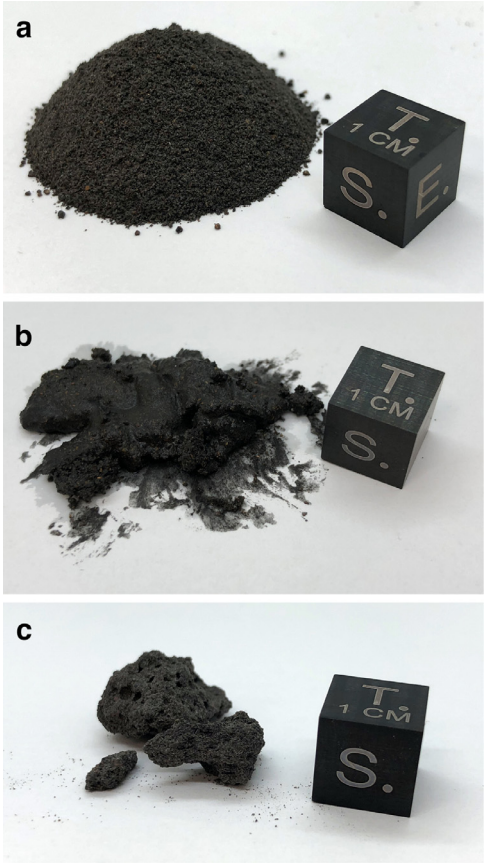

Fig. 2. Processing MGS-1 primary phases. (a) Mixed primary phases, including plagioclase, basaltic glass, pyroxene, olivine and magnetite. (b) Paste formed from primary phases, water, and sodium metasilicate. (c) Resulting solid cobble formed after the paste is dried and solidified.

original Saddleback Basalt. Quantitative mineralogical analysis is not available for either JSC Mars-1, MMS, MMS-1, or MMS-2, although this is not really feasible for JSC Mars-1 due to its mostly X-ray amorphous character.

There are a number of important differences between these older Mars simulants and new in-situ measurements of martian regolith. In terms of crystallinity, JSC Mars-1 is mostly X-ray amorphous, while MMS, MMS-1 and MMS-2 are nearly 100% crystalline. In contrast, martian soils are a subequal mixture of crystalline and amorphous phases, as revealed by the CheMin instrument on the Mars Science Laboratory (MSL) Curiosity rover (Bish et al., 2013; Blake et al., 2013; Dehouck et al., 2014; Achilles et al., 2017). JSC Mars-1 is extremely hygroscopic, contains >20 wt% H_2O at ambient conditions (Allen et al., 1998), and is known to contain significant organic carbon as well (Wamelink et al., 2014). Most of the older simulant varieties contain almost no sulfur, whereas martian regolith contains up to 6 wt % SO_3 (assuming all S is in the form of sulfate; Yen et al., 2005; Ming and Morris, 2017). As noted above, the MMS-2 simulant is spiked with sulfates and other phases to resolve discrepancies in bulk chemistry, but the composition on the package confusingly lists both mineral percentages and wt% oxides in the same table, summing them to 100%.

Other Mars simulants have also been developed based on terrestrial basalts, natural weathering profiles, and commercial sand products. Nørnberg et al. (2009) described Salten Skov 1, a magnetic dust analog composed mostly of crystalline iron oxides. Schuerger et al. (2012) created a series of analog soils by spiking a terrestrial basalt with various salts and carbonates; they used them to test the survival of microbial colonies in martian conditions. Other countries have developed Mars simulants, including a series of nepheline and quartz sands as geotechnical simulants for the European Space Agency (Gouache et al., 2011), terrestrial basalt spiked with magnetite and hematite for China's Mars exploration program (Zeng et al., 2015), and basalt mixed with volcanic glass in New Zealand (Scott et al., 2017). These simulants have not yet been widely distributed or adopted.

1.2. New insights on martian regolith

The surface of Mars is covered by an unconsolidated regolith produced by the combined action of impact comminution, physical erosion by wind, water, and lava, and chemical weathering by fluids and oxidants (mostly early in the history of Mars) (McCauley, 1973; Malin and Edgett, 2000; Golombek and Bridges, 2000; Goetz et al., 2005; Yen et al., 2005; Murchie et al., 2009). The finest particle size fraction, known as dust, is lofted high into the atmosphere by winds and is implicated in global storm patterns (Toon et al., 1977). Martian dust is somewhat chemically distinct from the underlying soil, with a larger component of npOx responsible for its ochre hue (Morris et al., 2001; Berger et al., 2016). Presumably the dust was or still is derived from regolith-forming processes, such that martian dust is a more “processed” and oxidized version of the underlying coarser soil. The soil itself has a basaltic composition (Yen et al., 2005; Ming and Morris, 2017), derived from a globally basaltic crust (McSween et al., 2009).

Martian soils have been examined in-situ at seven locations by landers and rovers, with supplemental information from orbital remote sensing. Soil major element chemistry and mineralogy are quite similar at the Spirit, Opportunity, and Curiosity landing sites (Yen et al., 2013; Ming and Morris, 2017), supporting the presence of a global basaltic soil that may be locally to regionally enriched in rarer evolved volcanic compositions (e.g., Christensen et al., 2005) or alteration phases (e.g., Squyres et al., 2008). However, the three landing sites compared in Yen et al. (2013) are all from sulfur-rich terrains (Karunatillake et al., 2014), and a true global average may have less sulfur-bearing minerals consistent with this bulk chemistry constraint. Regardless, the MGS-1 standard is modeled on the Rocknest windblown soil at Gale crater, with supplemental information from measurements by other landed and orbital assets. Rocknest is the best-characterized martian soil to date (Bish et al., 2013; Blake et al., 2013; Leshin et al., 2013; Minitti et al., 2013; Archer et al., 2014; Sutter et al., 2017; Achilles et al., 2017), and based on currently available data its chemical similarity to soils at disparate landing sites makes it an appropriate reference material from which to develop a new simulant standard.

2. The MGS-1 standard

2.1. Design philosophy

Our general approach to designing asteroid and planetary simulants is to start from the mineralogy, because minerals are the basic building blocks of planetary materials. By starting with the correct mineral constituents, many of the derived properties (spectral, volatile, etc.) should closely match the reference material, with adjustments made as necessary based on analyzing initial prototypes. Geomechanical properties are important for simulant behavior, and these can be adjusted easily by developers or end users through careful sieving (e.g., Battler and Spray, 2009). We applied a mineral-based design philosophy for the MGS-1 standard, based on X-ray Diffraction (XRD) analyses for the crystalline portion of the Rocknest soil (Bish et al., 2013; Achilles et al., 2017), and inferences for the amorphous component (Bish et al., 2013; Dehouck et al., 2014; Achilles et al., 2018).

2.2. Mineral recipe and calculated bulk chemistry

2.2.1. Crystalline fraction

The crystalline fraction of Rocknest is well constrained by XRD (Bish et al., 2013; Achilles et al., 2017). These measurements provide quantitative mass fractions of all minerals present at ~1 wt% or greater, and crystal chemistry constraints for major minerals from unit cell parameters and/or site occupancy. The detected crystalline phases in Rocknest include plagioclase, pyroxene, olivine, magnetite, anhydrite, hematite, ilmenite, and quartz (Bish et al., 2013; Achilles et al., 2017). We adopt most of the same mineral proportions reported by Achilles et al. (2017) (Table 1). For simplicity and sourcing concerns we do not include ilmenite or quartz in the MGS-1 standard, which were near the detection limits of CheMin. Magnetite, anhydrite and hematite were also near the detection limit, but magnetite is important for magnetic properties, anhydrite for sulfur contents, and hematite for pigmenting properties.

Table 1
Mineral recipe for the MGS-1 standard.

Component	MGS-1 (wt.%)	Rocknest crystalline + amorphous[a]
Crystalline phases	65.0%	65.0%
Plagioclase	27.1	26.3
Pyroxene	20.3	19.7
Olivine	13.7	13.3
Magnetite	1.9	1.8
Hematite	1.1	1.0
Anhydrite	0.9	0.9
Quartz	0.0	0.8
Ilmenite	0.0	0.9
Amorphous phases	35.0%	35.0%[b]
Basaltic Glass	22.9	–
Hydrated Silica (Opal)	5.0	–
Mg-sulfate[c]	4.0	–
Ferrihydrite	1.7	–
Fe-carbonate[d]	1.4	–
Sum	100.0	100.0%

[a] From Achilles et al. (2017), their Table 1.
[b] The total amorphous content is listed in Achilles et al. (2017), but not the constituents.
[c] In the prototype simulants we added crystalline epsomite.
[d] In the prototype simulants we added crystalline siderite.

Table 2
Bulk major element chemistry for Rocknest (RN) and the MGS-1 simulant.

Oxide	RN bulk[a]	Calc. MGS-1[b]	RN amorph.[c]	Calc. MGS-1 amorph.[b]	MGS-1 prototype
SiO_2	43.0	48.3	34.2	47.0	50.8
TiO_2	1.2	0.2	2.1	0.6	0.3
Al_2O_3	9.4	9.5	5.4	7.0	8.9
Cr_2O_3	0.5	0.1	1.4	0.2	0.1
FeO_T	19.2	16.9	23.0	21.0	13.3
MnO	0.4	0.1	1.2	0.2	0.1
MgO	8.7	12.1	4.0	9.9	16.7
CaO	7.3	6.7	4.4	4.5	3.7
Na_2O	2.7	2.6	3.3	1.0	3.4
K_2O	0.5	0.1	1.4	0.3	0.3
P_2O_5	1.0	0.2	2.7	0.6	0.4
SO_3	5.5	3.2	13.9	7.7	2.1
Cl	0.7	0.0	2.0	0.0	–
SUM	100.1	100.0	99.9	100.0	100.0

[a] From Achilles et al. (2017), their Table 6.
[b] Calculated using the mineral recipe in Table 1, and idealized mineral formulas with silicate crystal chemistries from Achilles et al. (2017).
[c] From Achilles et al. (2017), their Table 8.

2.2.2. Amorphous fraction

Poorly crystalline and/or X-ray amorphous material makes up at least 21–22% of the Rocknest soil sample by weight (Dehouck et al., 2014), and it is still not entirely clear what this material is. Dehouck et al, (2014), Morris et al. (2015), and Achilles et al. (2017) have refined the elemental chemistry of the amorphous component using a mass balance approach (Table 2), showing that it is deficient in SiO_2, Al_2O_3, and CaO, and enriched in SO_3 and H_2O compared to the bulk soil. The amorphous component cannot easily be explained by a single phase, and it is likely a mixture of silica-bearing phases such as basaltic glass and opaline silica, npOx phases like ferrihydrite (Dehouck et al., 2014, 2017), and one or more sulfate species like magnesium sulfate (Achilles et al., 2018), ferric sulfate (Sklute et al., 2015), or sulfate anions adsorbed onto other phases (McAdam et al., 2014; Rampe et al., 2016). Crystalline carbonates were not detected in Rocknest, but evolved gas analysis suggests one or more carbonate-bearing phases is present (Sutter et al., 2017). Other components not uniquely detectable by XRD could include allophane, hisingerite, and gels/protoclays.

Despite this inherent uncertainty, we chose to adopt the amorphous phases from Achilles et al. (2018), based on coupled constraints from XRD and geochemistry (Table 1). This includes basaltic glass, hydrated silica, ferrihydrite, and magnesium sulfate. We also added iron carbonate, consistent with the evolved gas analysis from Sutter et al. (2017). This results in a parsimonious and easy-to-source selection of phases covering the major anion groups, instead of including every possible amorphous phase that has been proposed. In terms of the silica-bearing portion of the amorphous component, we note that glass on Mars has been severely underappreciated in the past, and has been dismissed by some authors interpreting the CheMin results. But glassy spherules are clearly observed in soils at both the Phoenix and Curiosity landing sites (Goetz et al., 2010; Minitti et al., 2013), and the widespread presence of glass is supported by orbital investigations (Horgan and Bell, 2012; Cannon and Mustard, 2015; Cannon et al., 2017; Horgan et al., 2017). Magnesium sulfate and iron carbonate, two of the five “amorphous” species in MGS-1, were added to the prototype simulants in the crystalline state as epsomite and siderite, respectively. These species can be synthesized in amorphous form by evaporating appropriate solutions in vacuum (e.g., Sklute et al., 2015), but they are prone to recrystallize in normal laboratory conditions. The hydrated silica component has been described as Opal A (Achilles et al., 2018), but natural opal is extremely expensive and we used Diatomaceous Earth in the prototypes as the hydrated silica component.

2.2.3. Oxychlorines and nitrates

Oxychlorine species are present in martian soil and could include (per)chlorate salts (Hecht et al., 2009; Sutter et al., 2017) and/or peroxide species (Clancy et al., 2004; Crandall et al., 2017). Nitrates are also present (Stern et al., 2015). Perchlorates in particular have received significant attention because of their possible toxicity, and they will present a challenge and opportunity for human exploration in the future (Davila et al., 2013). No crystalline (per)chlorate salts were detected in Rocknest above the ~1 wt% detection limit, but evolved O_2 and HCl were detected and suggest (per)chlorates are present in some form (Archer et al., 2014). We included crystalline nitrate and perchlorate salts in some of our initial prototypes designed for agricultural studies, but do not include them in the root MGS-1 standard.

2.2.4. Bulk chemistry

Because MGS-1 is a mineralogical standard, the bulk chemistry of simulants created from the standard will change based on the crystal chemistry of the minerals used. Table 2 lists the elemental chemistry of the bulk Rocknest soil and the isolated amorphous component from Achilles et al. (2017). From the mineral recipe (Table 1), we calculated an estimated chemical composition for MGS-1 simulants using idealized chemical formulas for the constituent phases, including the actual Mars crystal chemistries for plagioclase, pyroxene and olivine from Achilles et al. (2017) that are updated from Bish et al. (2013) and Morris et al. (2015). Average martian crust (Taylor and McLennan, 2009) was used for the basaltic glass composition in the calculation. This results in an elemental chemistry within ~4 wt% of bulk Rocknest for all major oxide species, with SiO_2 the largest outlier in absolute terms. It can be difficult to impossible to find large quantities of terrestrial minerals with crystal chemistries appropriate for Mars (especially olivine and pyroxene), such that actual MGS-1 based simulants will deviate from the calculated chemistry depending on the specific silicates used. More effort put into sourcing accurate mineral chemistries (or combinations of endmembers) will result in a more accurate elemental chemistry for the final product.

2.2.5. Additional considerations

Perfect simulants do not exist, and there are almost certainly trace mineral species present in martian soil that aren't represented in MGS-1: these could include phosphates, sulfides, chromates, oxalates, and other rare species. Additional phases may be present in an amorphous or poorly-crystalline state, as discussed above. As well, silicate minerals are likely shocked to various degrees on Mars, whereas the basic MGS-1 standard does not account for this. Some phases are detected only in localized regions on Mars like clays (e.g., Poulet et al., 2005), halide salts (e.g., Osterloo et al., 2008), and potassic feldspar (e.g., Le Deit et al., 2016), and would be expected to be mixed into regional soils, but likely not on a global scale at detectable (>1 wt%) amounts. In Section 5.2 we discuss how different versions of MGS-1 could be created to simulate these regional soils.

3. Prototype simulant production

Using the MGS-1 mineral standard, we created prototype regolith simulants and analyzed them using a variety of instrumental techniques. The production methods and results are described below.

3.1. Source materials

We have built up a large library of source materials as part of ongoing work developing high-fidelity asteroid simulants (Britt et al., Simulated asteroid materials based on carbonaceous chondrite mineralogies, *manuscript in preparation*). These phases have been crushed into powders and analyzed by XRD, VNIR spectroscopy, and X-ray Fluorescence (XRF) to verify their identity and detect any contaminants present. The source materials for the MGS-1 prototypes come from a

combination of these existing stocks and newly acquired materials. We recommend natural mined sources for the major silicates. Basaltic glass is available commercially, although it is often in a fibrous form that is not ideal for producing simulants. Many of the other source materials are available in pure forms at low cost (Mg-sulfate as Epsom salt, Fe-carbonate as ferrous carbonate, magnetite as black iron oxide, and hematite as red iron oxide). Ferrihydrite is available commercially under the name "High capacity ferric granular oxide", and hydrated silica as "Diatomaceous Earth".

The crystal chemistry of the major silicates (plagioclase, pyroxene and olivine) differs between the prototype simulants and actual Rocknest measurements. Unit cell parameters for Rocknest minerals indicate An_{40} plagioclase (Achilles et al., 2017), a mixture of augite and pigeonite (Bish et al., 2013), and Fo_{58} olivine (Achilles et al., 2017). In the prototype simulants we used combinations of anorthosite from the Stillwater complex, labradorite from Madagascar, and feldspar from North Carolina for the plagioclase component; a single bronzite-variety pyroxene from Brazil, and the highly forsteritic San Carlos olivine. Measured chemistries for the silicates are included in Supplementary Table 1.

3.2. Simulant preparation

To create simulants using the MGS-1 standard, we mixed mineral components in the proportions listed in Table 1. If the mineral powders are simply mixed together dry, the resulting material will not accurately represent the regolith-forming process on Mars, where basalt is physically and chemically eroded to form soil. To address this, we used some of the same techniques for our asteroid simulants, where polymineralic fused solid "cobbles" are created then mechanically ground to achieve a more natural texture and particle size distribution. To create these cobbles, the plagioclase, pyroxene, olivine, basaltic glass, and magnetite were combined (Fig. 2(a)) and mixed with water and sodium metasilicate pentahydrate (a binder) in a 100:20:2 ratio by weight. Sodium metasilicate is not relevant to Mars, but this small amount is not expected to significantly affect the bulk properties of the simulant. It contributes 0.37 wt% excess SiO_2, 0.38 wt% excess Na_2O, and a maximum of 0.55 wt% excess H_2O, but much of this water is lost during heating. The mixture was combined and kneaded by hand to form a thick paste (Fig. 2(b)); for larger amounts a commercial stand mixer could also be used. The paste was then placed in a microwave oven to remove the water (time and power settings depend on the amount of paste). Upon heating and drying, the sodium metasilicate forms a polymer network that acts as a binder, such that the resulting cobbles are solid and quite hard (Fig. 2(c)). These cobbles were then ground (rock crushers, ball mills, or hand tools are sufficient) and mechanically stirred (by hand; cement mixers could be used for larger amounts) with the remaining secondary phases (hydrated silica, magnesium sulfate, ferrihydrite, anhydrite, siderite, and hematite) to create the final simulant (Fig. 1(b)). In the prototypes we sieved the final product to a <1 mm particle size, but this is highly adjustable and not an inherent property of the simulant.

3.3. Analyses

The prototype simulants were analyzed using a variety of bulk techniques. Results from these analyses were compared to relevant datasets from various in-situ and orbital Mars spacecraft measurements as appropriate. In terms of physical/grain properties, bulk density was measured by gently pouring a known mass of simulant into a graduated cylinder to measure its volume, and the particle size distribution was measured in triplicate at the Johnson Space Center ARES facilities using a Microtrac S3500 particle size analyzer with isopropyl alcohol as the medium. Bulk elemental chemistry of the simulant prototypes was measured at the UCF Materials Characterization Facility using a PANalytical Epsilion XRF operating in oxides mode. Spectral properties of the simulants were measured at UCF using an Analytical Spectrum Devices FieldSpec spectroradiometer from 320 to 2550 nm. This range covers typical measurements made by rovers and orbital remote sensing platforms at Mars. The JSC Mars-1, MMS-1 and MMS-2 simulants were measured at the same time for comparison. All the simulants were ground and dry-sieved to the same 45–75 μm size fraction. Combined thermogravimetry (TG) and evolved gas analysis (EGA) was measured at the ARES facilities using a Labsys EVO differential scanning calorimeter/thermal gravimeter connected to a ThermoStar quadrupole mass spectrometer configured to operate similarly to the MSL Sample Analysis at Mars (SAM) instrument. Analyses were done under a 30 mbar helium atmosphere, and the sample was heated from ambient to 1000 °C at a ramp rate of 35 °C/min.

4. Results

A photograph of the MGS-1 based simulant is shown in Fig. 1(b), compared with an approximately true color image of the Rocknest windblown soil (Fig. 1(a)) taken by the MSL Mars Hand Lens Imager (MAHLI) (Minitti et al., 2013). MGS-1 has a similar burnt umber color to Rocknest, mostly caused by the mixture of gray to black silicates and the ferrihydrite and hematite, which act as strong pigments.

4.1. Physical properties

The basic physical properties of the MGS-1 prototypes are consistent with the limited data available from Mars rovers and landers. The bulk density of the prototype simulant is 1.29 g/cm^3; by comparison, soils at the Pathfinder landing site had an estimated bulk density of 1.07–1.64/cm^3 (Moore et al., 1999), and drift material at the Viking 1 landing site had an estimated bulk density of 1.15 ± 0.15 g/cm^3 (Moore and Jakosky, 1989), although the lower gravity may affect bulk density somewhat. We could not find a published estimate of density or porosity for the Rocknest windblown soil. Pristine martian basalts have much higher grain densities (>3 g/cm^3), but this density is lowered through physical and chemical weathering processes during regolith formation. Fig. 3 shows the particle size distribution for the prototypes that were sieved to <1 mm. The distribution is somewhat bimodal, likely due to the secondary phases that form a distinct, finer distribution than the crushed polymineralic silicate particles. The mean grain size (by volume) is 122 μm. Minitti et al. (2013) found the interior of the Rocknest sand shadow had $<10\%$ of particles 0.5–2 mm in diameter, 40–60% of particles between 100–150 μm, and 30–50% of finer grains. Grains <31 μm could not be resolved by MAHLI, but at the Phoenix landing site Pike et al. (2011) combined optical and atomic

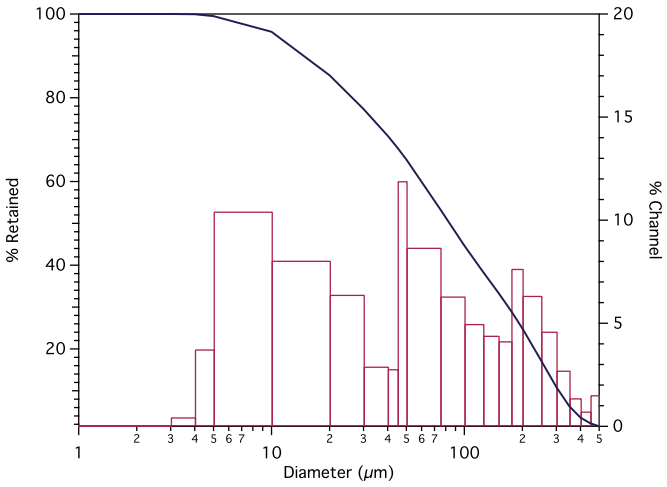

Fig. 3. Particle size analysis. The solid line shows the cumulative distribution, and the bars show the fraction of grains in each of the channels.

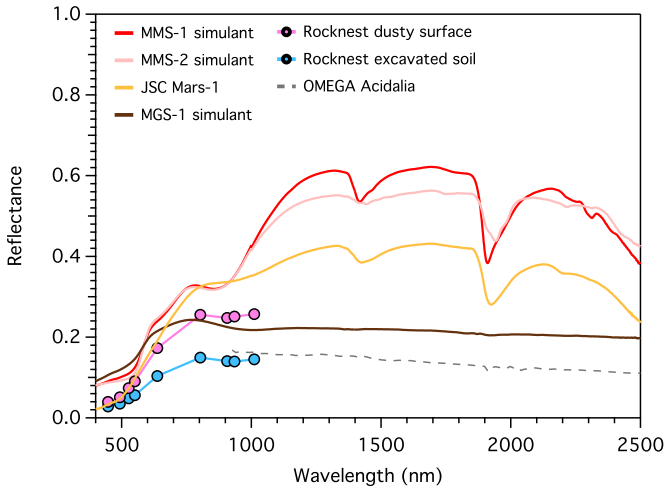

Fig. 4. Spectral comparison of the MGS-1 simulant prototype, previous Mars simulants, and remotely sensed data from Curiosity and OMEGA. Mastcam data (filled circles) were reproduced from Fig. 5 in Wellington et al. (2017), and OMEGA data courtesy of R. Milliken. None of the spectra have been offset or scaled.

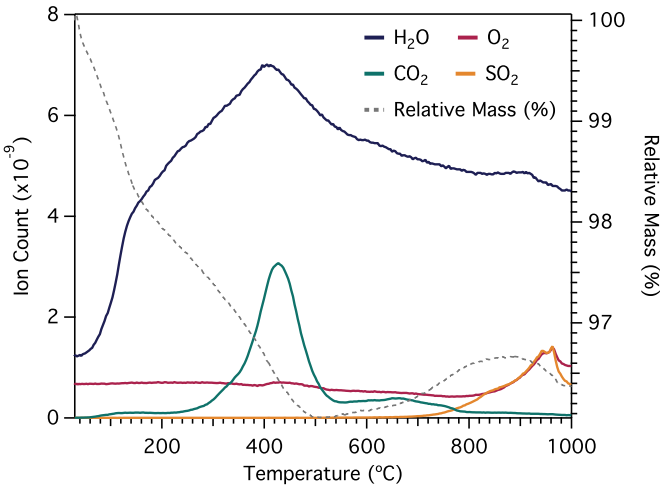

Fig. 5. Combined thermogravimetry and evolved gas analysis of MGS-1 prototype, performed in at SAM-like conditions.

force microscopy to analyze soils, finding <1 vol.% of grains less than 4 μm in diameter. This is consistent with the MGS-1 prototype.

4.2. Bulk chemistry

Table 2 lists the bulk chemistry of the prototype simulants as measured by XRF (rightmost column), in addition to the forward-calculated estimates for the MGS-1 standard described above. As expected, there are deviations from the Rocknest measurements due to the crystal chemistry of the silicate minerals used in the prototypes. MgO and FeO are most affected. For future versions of MGS-1 simulants, the best way to achieve a more accurate bulk chemistry will be to use a more realistic olivine and pyroxene compositions, or to physically combine end-member phases in appropriate proportions.

4.3. Spectral properties

Fig. 4 shows the reflectance spectrum of the MGS-1 prototype simulant compared to previous simulants, and to rover and orbital data from Mars. At shorter wavelengths, the MGS-1 based simulant is broadly similar in shape and albedo to the Rocknest spectra acquired by Mastcam (Wellington et al., 2017). In particular, the absorptions and shoulders are consistent between 400 and 1100 nm, associated with (1) Fe^{2+}–Fe^{3+} and Fe–O charge transfer at visible wavelengths, and (2) Fe^{2+} crystal field splitting in olivine and pyroxene near 1000 nm. At longer wavelengths, the simulant spectrum is similar to low albedo regions on Mars imaged by the Observatoire pour la Minéralogie, l'Eau, les Glaces, et l'Activité (OMEGA) orbital spectrometer (Milliken et al., 2007). However, the simulant is brighter at all wavelengths: this could be caused by differing crystal chemistry (fayalite is much darker than forsterite), the specific nature of the amorphous component on Mars, and shock darkening/brecciation effects (Cannon et al., 2015).

The other Mars simulants measured, JSC Mars-1, MMS-1 and MMS-2, are not close matches to Rocknest or low albedo terrains measured by OMEGA. All these simulants have dramatically higher albedos than the remote measurements, with strong H_2O- and OH-related absorptions at 1400 and 1900 nm and significant structure from 1900–2500 nm indicative of multiple different alteration phases present in significant amounts. We did not measure the original MMS simulant described by Peters et al. (2008), but the spectra shown in their Fig. 4 (no absolute reflectance scale) and in Beegle et al. (2007) do not resemble the MMS-1 or MMS-2 simulants, and are more representative of actual Mars materials.

4.4. Thermogravimetry and evolved gas analysis

The MGS-1 prototype lost 3.9% relative mass between 30 and 500 °C, with a broad release of H_2O that has superimposed structure (Fig. 5). There was a sharp release of CO_2 related to the thermal breakdown of siderite, and at higher temperatures, releases of SO_2 and O_2 around 950 °C are related to the thermal breakdown of Mg-sulfate (Fig. 5). Assuming siderite completely decomposes, the H_2O-related mass loss from 30 to 500 °C corresponds to 3.2 wt.% H_2O in MGS-1. In comparison, Allen et al. (1998) reported that JSC Mars-1 lost 21.1 wt.% (mostly water) when heated to 600 °C, while Peters et al. (2008) report that MMS lost 7.2 wt.% by 500 °C. The significant and unrealistic water contents of JSC Mars-1 were cited as a motivating factor in developing the original MMS simulant (Peters et al., 2008), and MMS has recently been augmented further to achieve even more realistic volatile release patterns (Archer et al., 2018). TG/EGA data are not available for MMS-1 or MMS-2, but judging from their spectral properties with strong OH- and H_2O-related absorptions (Fig. 3) these simulants have significant water contents on par with JSC Mars-1.

The volatile release pattern of MGS-1 is consistent with soils measured on Mars. The Thermal and Evolved Gas Analyzer instrument did not detect a low temperature water release in soil samples at the Phoenix landing site (Smith et al., 2009), but did detect a minor H_2O release starting at 295 °C and a major release starting at 735 °C. In contrast, the SAM instrument detected a broad H_2O release in Rocknest starting at low temperatures, finding 2.0 ± 1.3 wt.% total evolved water averaged over four runs (Archer et al., 2014). This is consistent with the 1.5 wt.% water equivalent hydrogen in the upper layer of Rocknest materials measured by DAN (Jun et al., 2013). The shape of the H_2O release in MGS-1 has more structure than Rocknest and continues rising to higher temperatures, but the total amount of evolved H_2O is similar, and compares favorably to past simulants. Rocknest also shows distinct CO_2 releases at 400 and 510 °C, and an SO_2 release between 700–750 °C (Leshin et al., 2013; Archer et al., 2014; Sutter et al., 2017). Gas releases attributed to (per)chlorate salts are observed in Rocknest (Archer et al., 2014; Sutter et al., 2017), but not in the measured MGS-1 prototypes where these species were not included.

5. Discussion

Simulants created using the MGS-1 standard are superior to previous martian simulants, and accurately capture advances in the understanding of real martian regolith in the 10 years since MMS was

described (Peters et al., 2008) and the 20 years since JSC Mars-1 debuted (Allen et al., 1998). The high fidelity of MGS-1 simulants is made possible by the mineralogy-based synthesis, where mostly pure, individual components are mixed together from scratch. This is in contrast to previous simulants, where a natural, roughly basaltic terrestrial material was found that superficially matched Mars in terms of spectral or bulk chemical properties. That is not to say these previous simulants have no value, especially where applications only require a bulk granular material that behaves somewhat similarly to actual regolith on Mars.

5.1. Applications

Simulants based on MGS-1 are appropriate to use for a variety of scientific and engineering-based investigations, as well as for testing flight hardware and developing in-situ resource utilization (ISRU) technology. For lunar simulants, NASA developed the concept of a fit-to-use matrix (Schrader et al., 2010), where various simulants are compared by describing applications for which they are or are not recommended. For example, the highlands simulant NU-LHT-1D was not recommended for drilling studies because of its fine particle size distribution, but was deemed appropriate for oxygen production studies. A simulant fit-to-use matrix is more relevant for the Moon because of the vast proliferation of different lunar simulants, at least 33 by our count. The situation for Mars is different, with fewer formally described simulants (http://sciences.ucf.edu/class/planetary-simulant-database/): the most prominent of these (MMS and JSC Mars-1) are no longer available outside of NASA, and the others have not yet been widely adopted. Nevertheless, without a formal fit-to-use matrix we can still list the various strengths and weaknesses of the MGS-1 standard in terms of different use cases.

MGS-1 simulants are most recommended in applications where mineralogy and volatile contents are important controlling factors. These include ISRU technology development, plant growth and astrobiology studies, human health assessments, and recurring slope lineae experiments, among others. JSC Mars-1 is not recommended for these applications because it has virtually none of the same minerals as actual Mars soil, and its volatile content (>20 wt.% H_2O) is highly unrealistic. The original MMS simulant, and some of the newer simulants (JMSS-1, UC Mars1) may be appropriate for some of these cases where accurate mineralogy is not critical. However, we caution against using MMS-1 or MMS-2 due to their lack of rigorous documentation and the discrepancies between these and the original MMS, as described above.

MGS-1 simulants are also recommended in applications for testing flight hardware such as drilling, where geomechanical properties are important. MGS-1 is appropriate for these cases because the synthesis method produces a “regolith” of polymineralic grains with an adjustable particle size distribution, instead of simply mixing dry powders together. However, the geomechanical properties of actual martian regolith are poorly constrained compared to returned lunar regolith that has been studied extensively on Earth. As well, in the prototypes we did not control for detailed aspects like particle shape that can be important in influencing geomechanical behavior, and our initial physical properties measurements in this study are limited. Other simulants, particularly lunar ones, have benefitted from detailed crushing protocols to replicate lunar geomechanical properties (e.g., Battler and Spray, 2009). At this time, we can only say that MGS-1 based simulants can likely be made to be as appropriate or more so for hardware testing compared to previous Mars simulants. Mojave Mars Simulant was developed specifically for geotechnical applications (Peters et al., 2008), and if the original version can be obtained it is recommended for these uses. Again, due to apparent changes between MMS and MMS-1/2, we do not recommend these simulants. Newer Mars simulants (JMSS-1, UC Mars1, ES-X) may also be appropriate for geotechnical applications. In order to improve the usefulness of Mars simulants for flight hardware tests, more detailed study of actual martian regolith is needed. Some of this may come from the InSight and ExoMars missions, which will hammer and drill deep into surface materials. In addition, it would be useful to conduct a rigorous testing and inter-comparison of martian simulants for physical properties (including thermophysical properties).

We do not recommend using MGS-1 simulants for detailed geochemical studies such as aqueous alteration experiments. This is due to the uncertainty in the exact amount and nature of the amorphous component in martian soils, and the difficulty in sourcing silicates on Earth with crystal chemistries appropriate for Mars. For these types of studies it may be better to use pure minerals in experiments, synthesize silicates from raw oxides, and/or to rely on geochemical modeling based on primary volcanic compositions from martian meteorites or rover measurements. In theory it is possible to create a small amount of extremely high fidelity regolith simulant that satisfies both mineral and chemical constraints simultaneously, but it is cost-prohibitive to make this kind of simulant in large quantities accessible to the community.

5.2. Availability and future development of MGS-1

We hope to avoid some of the pitfalls of past simulant production and move toward a more open and sustainable model. This starts with the general philosophy of the standard: MGS-1 essentially means any simulant created based on the mineralogy of average basaltic regolith on Mars, as captured by the mineral recipe in Table 1. While we have chosen to add the plagioclase, pyroxene and olivine separately in our prototypes, they could also be added in the form of basalt or ultramafic rocks provided the mineral proportions are accurate. The MGS-1 recipe can be updated in the future based on new analyses (for example, further refining the amorphous component; Achilles et al. (2018)) and exploration of new landing sites. In this way, there is no batch of MGS-1 to run out, but a general standard to follow. We intend to produce modest quantities of MGS-1 based simulant and distribute it to the community, but we also encourage others to re-create the same types of simulant using a similar standard. Indeed, a group at the Johnson Space Center is also developing a Rocknest-based version of the MMS simulant to be used for ISRU development (Archer et al., 2018).

NASA developed the concept of “root” and “branch” simulants for the Moon, where the root is a basic, well-characterized version of the simulant. Specialized branch versions can be derived from the root, either by the original developer or by end users. MGS-1 will benefit from the same scheme, where the recipe in Table 1 forms the basic root, and various branches can be created either by us or others. For example, clay-rich Noachian regolith, or perchlorate and nitrate-bearing agricultural soils can be created by adding the desired additional components to the root simulant. These may evolve into standardized simulants with version numbers to achieve better consistency, instead of each individual lab developing their own simulant recipe. We encourage others to develop branched versions of MGS-1 and add modifiers to the name as they see fit.

6. Conclusions

We developed a new standard for a Mars simulant, the MGS-1 Mars Global Simulant, based on the Rocknest soil examined by the Curiosity rover. Unlike previous simulants sourced from landscaping material, Mars Global is meant to be assembled ab initio from individual components to provide an accurate match to the mineralogy of martian regolith. The physical, chemical, spectral and volatile properties of prototype simulants based on MGS-1 are similar to measurements of Rocknest and other soils on Mars, and are an improvement over previous simulants. MGS-1 based simulants are recommended for a variety of applications including ISRU development, agriculture/astrobiology studies, and testing flight hardware. Modest amounts of simulant will be produced and made available to the community, but through an open source philosophy we encourage end users to freely replicate and modify the MGS-1 standard using the recipe and procedure described

here.

Acknowledgements

The authors would like to thank Richard Blair and Katerina Chagoya for help with ferrihydrite synthesis, Valerie Tu, Joanna Hogancamp and Elizabeth Rampe for running EGA and particle size analyses, and the MCF facility staff for help with instrumental analyses. Reviews from Elizabeth Rampe and an anonymous reviewer were constructive, helpful, and greatly improved the final manuscript.

Supplementary materials

Supplementary material associated with this article can be found, in the online version, at doi:10.1016/j.icarus.2018.08.019.

References

Achilles, C.N., Downs, R.T., Ming, D.W., Rampe, E.B., Morris, R.V., Treiman, A.H., Morrison, S.M., Blake, D.F., Vaniman, D.T., Ewing, R.C., Chipera, S.J., Yen, A.S., Bristow, T.F., Ehlmann, B.L., Gellert, R., Hazen, R.M., Fendrich, K.V., Craig, P.I., Grotzinger, J.P., Des Marais, D.J., Farmer, J.D., Sarrazin, P.C., Morookian, J.M., 2017. Mineralogy of an active eolian sediment from the Namib dune, Gale crater, Mars. J. Geophys. Res. 112, 2344–2361. https://doi.org/10.1002/2017JE005262.

Achilles, C.N., Downs, G.W., Downs, R.T., Morris, R.V., Rampe, E.B., Ming, D.W., Chipera, S.J., Blake, D.F., Vaniman, D.T., Bristow, T.F., Yen, A.S., Morrison, S.M., Treiman, A.H., Craig, P.I., Hazen, R.M., Tu, V.M., Castle, N., 2018. Amorphous phase characterization through X-ray diffraction profile modeling: Implications for amorphous phases in Gale crater rocks and soils. In: Proceedings of the Lunar and Planetary Science Conference, XLIX, 59 Abstract #2661.

Allen, C., Morris, R.V., Jager, K.M., Golden, D.C., Lindstrom, D.J., Lindstrom, M.M., Lockwood, J.P., 1998. Martian regolith simulant JSC Mars-1. In: Proceedings of the Lunar and Planetary Science Conference, XXIX, 29 Abstract #1690.

Archer Jr., P.D., Franz, H.B., Sutter, B., Arevalo Jr., R.D., Coll, P., Eigenbrode, J.L., Glavin, D.P., Jones, J.J., Leshin, L.A., Mahaffy, P.R., McAdam, A.C., McKay, C.P., Ming, D.W., Morris, R.V., Navarro-González, R., Niles, P., Pavlov, A., Squyres, S.W., Stern, J.C., Steele, A., Wray, J.J., 2014. Abundances and implications of volatile-bearing species from evolved gas analysis of the Rocknest Aeolian deposit, Gale Crater, Mars. J. Geophys. Res. 119, 237–254. https://doi.org/10.1002/2013JE004493.

Archer Jr., P.D., Hogancamp, J.V., Gruener, J.E., Ming, D.W., 2018. Augmenting the Mojave Mars Simulant to more closely match the volatile content of global martian soils based on Mars Science Laboratory results. In: Proceedings of the Lunar and Planetary Science Conference, XLIX, 47 Abstract #2806.

Arvidson, R.E., Bonitz, R.G., Robinson, M.L., Carsten, J.L., Volpe, R.A., Trebi-Ollennu, A., Mellon, M.T., Chu, P.C., Davis, K.R., Wilson, J.J., Shaw, A.S., Greenberger, R.N., Siebach, K.L., Stein, T.C., Cull, S.C., Goetz, W., Morris, R.V., Ming, D.W., Keller, H.U., Lemmon, M.T., Sizemore, H.G., Mehta, M., 2009. Results from the Mars Phoenix Lander Robotic Arm experiment. J. Geophys. Res. 114, E00E02. https://doi.org/10.1029/2009JE003408.

Battler, M.M., Spray, J.G., 2009. The Shawmere anorthosite and OB-1 as lunar highland regolith simulants. Planet. Space Sci. 57, 2128–2131. https://doi.org/10.1016/j.pss.2009.09.003.

Beegle, L.W., Peters, G.H., Mungas, G.S., Bearman, G.H., Smith, J.A., Anderson, R.C., 2007. Mojave martian simulant: a new martian soil simulant. In: Proceedings of the Lunar and Planetary Science Conference, XXXVIII, 38 Abstract #2005.

Bell III, J.F., Morris, R.V., Adams, J.B., 1993. Thermally altered palagonitic tephra: a spectral and process analog to the soil and dust of Mars. J. Geophys. Res 98, 3373–3385. https://doi.org/10.1029/92JE02367.

Berger, J.A., Schmidt, M.E., Gellert, R., Campbell, J.L., King, P.L., Flemming, R.L., Ming, D.W., Clark, B.C., Pradler, I., VanBommel, S.J.V., Minitti, M.E., Fairén, A.G., Boyd, N.I., Thompson, L.M., Perrett, G.M., Elliott, B.E., Desouza, E., 2016. A global Mars dust composition refined by the alpha-particle X-ray spectrometer in Gale Crater. Geophys. Res. Lett. 43, 67–75. https://doi.org/10.1002/2015GL066675.

Bernold, L.E., 1991. Experimental studies on mechanics of lunar excavation. J. Aerosp. Eng. 4, 9. https://doi.org/10.1061/(ASCE)0893-1321(1991)4:1(9).

Bish, D.L., Blake, D.V., Vaniman, D.T., Chipera, S.J., Morris, R.V., Ming, D.W., Treiman, A.H., Sarrazin, P., Morrison, S.M., Downs, R.T., Achilles, C.N., Yen, A.S., Bristow, T.F., Crisp, J.A., Morookian, J.M., Farmer, J.D., Rampe, E.B, Stolper, E.M., Spanovich, N., MSL Science Team, 2013. X-ray diffraction results from Mars science laboratory: mineralogy of rocknest at Gale Crater. Science 341, 1238932. https://doi.org/10.1126/science.1238932.

Blake, D.F., Morris, R.V., Kocurek, G., Morrison, S.M., Downs, R.T., Bish, D., Ming, D.W., Edgett, K.S., Rubin, D., Goetz, W., Madsen, M.B., Sullivan, R., Gellert, R., Campbell, I., Treiman, A.H., McLennan, S.M., Yen, A.S., Grotzinger, J., Vaniman, D.T., Chipera, S.J., Achilles, C.N., Rampe, E.B., Sumner, D., Meslin, P.-Y., Maurice, S., Forni, O., Gasnault, O., Fisk, M., Schmidt, M., Mahaffy, P., Leshin, L.A., Glavin, D., Steele, A., Freissinet, C., Navarro-González, R., Yingst, R.A., Kah, L.C., Bridges, N., Lewis, K.W., Bristow, T.F., Farmer, J.D., Crism, J.A., Stolper, E.M., Des Marais, D.J., Sarrazin, P., MSL Science Team, 2013. Curiosity at Gale Crater, Mars: characteriztion and analysis of the rocknest sand shadow. Science 341, 1239505. https://doi.org/10.1126/science.1239505.

Cannon, K.M., Mustard, J.F., 2015. Preserved glass-rich impactites on Mars. Geology 43, 635–638. https://doi.org/10.1130/G36953.1.

Cannon, K.M., Mustard, J.F., Agee, C.B., 2015. Evidence for a widespread basaltic breccia component in the martian low-albedo regions from the reflectance spectrum of Northwest Africa 7034. Icarus 252, 150–153. https://doi.org/10.1016/j.icarus.2015.01.016.

Cannon, K.M., Mustard, J.F., Parman, S.W., Sklute, E.C., Dyar, M.D., Cooper, R.F., 2017. Spectral properties of martian and other planetary glasses and their detection in remotely sensed data. J. Geophys. Res. 122, 249–268. https://doi.org/10.1002/2016JE005219.

Christensen, P.R., McSween Jr., H.Y., Bandfield, J.L., Ruff, S.W., Rogers, A.D., Hamilton, V.E., Gorelick, N., Wyatt, M.B., Jakosky, B.M., Kieffer, H.H., Malin, M.C., Moersch, J.E., 2005. Evidence for magmatic evolution and diversity on Mars from infrared observations. Nature 436, 504–509. https://doi.org/10.1038/nature03639.

Clancy, R.T., Sandor, B.J., Moriarty-Schieven, G.H., 2004. A measurement of the 362GHz absorption line of Mars atmospheric H_2O_2. Icarus 168, 116–121. https://doi.org/10.1016/j.icarus.2003.12.003.

Crandall, P.B., Góbi, S., Gillis-Davis, J., Kaiser, R.I., 2017. Can perchlorates be transformed to hydrogen peroxide (H_2O_2) products by cosmic rays on the martian surface? J. Geophys. Res. 122, 1880–1892. https://doi.org/10.1002/2017JE005329.

Davila, A.F., Willson, D., Coates, J.D, McKay, C.P., 2013. Perchlorate on Mars: a chemical hazard and a resource for humans. Int. J. Astrobiol. 12, 321–325. https://doi.org/10.1017/S1473550413000189.

de Vera, J.-P., Horneck, G., Rettberg, P., Ott, S., 2004. The potential of the lichen symbiosis to cope with the extreme conditions of outer space II: germination capacity of lichen ascospores in response to simulated space conditions. Adv. Space Res. 33, 1236–1243. https://doi.org/10.1016/j.asr.2003.10.035.

Dehouck, E., McLennan, S.M., Meslin, P.-Y., Cousin, A., 2014. Constraints on abundance, composition, and nature of X-ray amorphous components of soils and rocks at Gale Crater, Mars. J. Geophys. Res. 119, 2640–2657. https://doi.org/10.1002/2014JE004716.

Dehouck, E., McLennan, S.M., Sklute, E.C., Dyar, M.D., 2017. Stability and fate of ferrihydrite during episodes of water/rock interactions on early Mars: an experimental approach. J. Geophys. Res. 122, 358–382. https://doi.org/10.1002/2016JE005222.

Evans, D.L., Adams, J.B., 1979. Comparison of Viking Lander multispectral images and laboratory reflectance spectra of terrestrial samples. In: Proceedings of the 10th Lunar and Planetary Science Conference, pp. 1829–1834.

Goetz, W., Bertelsen, P., Binau, C.S., Gunnlaugsson, H.P., Hviid, S.F., Kinch, K.M., Madsen, D.E, Madsen, M.B., Olsen, M., Gellert, R., Klingelhöfer, G., Ming, D.W., Morris, R.V., Rieder, R., Rodinov, D.S., de Souza Jr., P.A., Schröder, C., Squyres, S.W., Wdowiak, T., Yen, A., 2005. Indication of drier periods on Mars from the chemistry and mineralogy of atmospheric dust. Nature 436, 62–65. https://doi.org/10.1038/nature03807.

Goetz, W., Pike, W.T., Hviid, S.F., Madsen, M.B., Morris, R.V., Hecht, M.H., Staufer, U., Leer, K., Sykulska, H., Hemmig, E., Marshall, J., Morookian, J.M., Parrat, D., Vijendran, S., Bos, B.J., El Maarry, M.R., Keller, H.U., Kramm, R., Markiewicz, W.J., Drube, L., Blaney, D., Arvidson, R.E., Bell III, J.F., Reynolds, R., Smith, P.H., Woida, P., Woida, R., Tanner, R., 2010. Microscopy analysis of soils at the Phoenix landing site, Mars: classification of soil particles and description of their optical and magnetic properties. J. Geophys. Res. 115, E00E22. https://doi.org/10.1029/2009JE003437.

Golombek, M.P., Bridges, N.T., 2000. Erosion rates on Mars and implications for climate change: constraints from the Pathfinder landing site. J. Geophys. Res. 105, 1841–1853. https://doi.org/10.1029/1999JE001043.

Gouache, T.P., Patel, N., Brunskill, C., Scott, G.P., Saaj, C.M., Matthews, M., Cui, L., 2011. Soil simulant sourcing for the ExoMars rover testbed. Planet. Space Sci. 59, 779–787. https://doi.org/10.1016/j.pss.2011.03.006.

Hecht, M.H., Kounaves, S.P., Quinn, R.C., West, S.J., Young, S.M.M., Ming, D.W., Catling, D.C., Clark, B.C., Boynton, W.V., Hoffman, J., DeFlores, L.P., Gospodinova, K., Kapit, J., Smith, P.H., 2009. Detection of perchlorate and the soluble chemistry of martian soil at the phoenix lander site. Science 325, 64–67. https://doi.org/10.1126/science.1172466.

Horgan, B., Bell III, J.F., 2012. Widespread weathered glass on the surface of Mars. Geology 40, 391–394. https://doi.org/10.1130/G32755.1.

Horgan, B.H.N., Smith, R.J., Cloutis, E.A., Mann, P., Christensen, P.R., 2017. Acidic weathering of basalt and basaltic glass: 1. Near-infrared spectra, thermal infrared spectra, and implications for Mars. J. Geophys. Res. 122, 172–202. https://doi.org/10.1002/2016JE005111.

Jun, I., Mitrofanov, I., Litvak, M.L., Sanin, A.B., Kim, W., Behar, A., Boynton, W.V., DeFlores, L., Fedosov, F., Golovin, D., Hardgrove, C., Harshman, K., Kozyrev, A.S., Kuzmin, R.O., Malakhov, A., Mischna, M., Moersch, J., Mokrousov, M., Nikiforov, S., Shvetsov, V.N., Tate, C., Tret'yakov, V.I., Vostrukhin, A., 2013. Neutron background environment measured by the Mars Science Laboratory's Dynamic Albedo of Neutrons instrument during the first 100 sols. J. Geophys. Res. 118, 2400–2412. https://doi.org/10.1002/2013JE004510.

Karunatillake, S., Wray, J.J., Gasnault, O., McLennan, S.M., Rogers, A.D., Squyres, S.W., Boynton, W.V., Skok, J.R., Ojha, L., Olsen, N., 2014. Sulfates hydrating bulk soil in the Martian low and middle latitudes. Geophys. Res. Lett. 41, 7987–7996. https://doi.org/10.1002/2014GL061136.

Le Deit, L., Mangold, N., Forni, O., Cousin, A., Lasue, J., Schröder, S., Wiens, R.C., Sumner, D., Fabre, C., Stack, K.M., Anderson, R.B., Blaney, D., Clegg, S., Dromart, G., Fisk, M., Gasnault, O., Grotzinger, J.P., Gupta, S., Lanza, N., Le Mouélic, S., Maurice, S., McLennan, S.M., Meslin, P.-Y., Nachon, M., Newsom, H., Payré, V., Rapin, W., Rice, M., Sautter, V., Treiman, A.H., 2016. The potassic sedimentary rocks in Gale Crater, Mars, as seen by ChemCam on board Curiosity. J. Geophys. Res. 121,

784–804. https://doi.org/10.1002/2015JE004987.
Leshin, L.A., Mahaffy, P.R., Webster, C.R., Cabane, M., Coll, P., Conrad, P.G., Archer Jr., P.D., Atreya, S.K., Brunner, A.E., Buch, A., Eigenbrode, J.L., Flesch, G.J., Franz, H.B., Freissinet, C., Glavin, D.P., McAdam, A.C., Miller, K.E., Ming, D.W., Morris, R.V., Navarro-González, R., Niles, P.B., Owen, T., Pepin, R.O., Squyres, S., Steele, A., Stern, J.C., Summons, R.E., Sumber, D.Y., Sutter, B., Szopa, C., Teinturier, S., Trainer, M.G., Wray, J.J., Grotzinger, J.P., MSL Science Team, 2013. Volatile, isotope, and organic analysis of martian fines with the Mars curiosity rover. Science 341, 1238937. https://doi.org/10.1126/science.1238937.
Malin, M.C., Edgett, K.S., 2000. Sedimentary rocks of early Mars. Science 290, 1927–1937. https://doi.org/10.1126/science.290.5498.1927.
McAdam, A.C., Franz, H.B., Sutter, B., Archer Jr., P.D., Freissinet, C., Eigenbrode, J.L., Ming, D.W., Atreya, S.K., Bish, D.L., Blake, D.F., Bower, H.E., Brunner, A., Buch, A., Glavin, D.P., Grotzinger, J.P., Mahaffy, P.R., McLennan, S.M., Morris, R.V., Navarro-González, R., Rampe, E.B., Squyres, S.W., Steele, A., Stern, J.C., Sumner, D.Y., Wray, J.J., 2014. Sulfur-bearing phases detected by evolved gas analysis of the Rocknest Aeolian deposit, Gale Crater, Mars. J. Geophys. Res. 119, 373–393. https://doi.org/10.1002/2013JE004518.
McCauley, J.F., 1973. Mariner 9 evidence for wind erosion in the equatorial and mid-latitude regions of Mars. J. Geophys. Res. 78, 4123–4137. https://doi.org/10.1029/JB078i020p04123.
McSween Jr., H.Y., Taylor, G.J., Wyatt, M.B., 2009. Elemental composition of the martian crust. Science 324, 736–739. https://doi.org/10.1126/science.1165871.
Milliken, R.E., Mustard, J.F., Poulet, F., Jouglet, D., Bibring, J.-P., Gondet, B., Langevin, Y., 2007. Hydration state of the Martian surface as seen by Mars express OMEGA: 2. H_2O content of the surface. J. Geophys. Res. 112, E08S07. https://doi.org/10.1029/2006JE002853.
Ming, D.W., Morris, R.V., 2017. Chemical, mineralogical, and physical properties of martian dust and soil. Dust in the Atmosphere of Mars and Its Impact on Human Exploration Workshop Abstract #6027. https://www.hou.usra.edu/meetings/marsdust2017/.
Minitti, M.E., Kah, L.C., Yingst, R.A., Edgett, K.S., Anderson, R.C., Beegle, L.W., Carsten, J.L., Deen, R.G., Goetz, W., Hardgrove, C., Harker, D.E., Herkenhoff, K.E., Hurowitz, J.A., Jandura, L., Kenney, M.R., Kocurek, G., Krezoski, G.M., Kuhn, S.R., Limonadi, D., Lipkaman, L., Madsen, M.B., Olson, T.S., Robinson, M.L., Rowland, S.K., Rubin, D.M., Seybold, C., Schieber, J., Schmidt, M., Sumner, D.Y., Tompkins, V.V., Van Beek, J.J., Van Beek, T., 2013. MAHLI at the Rocknet sand shadow: science and science-enabling activities. J. Geophys. Res. 118, 2338–2360. https://doi.org/10.1002/2013JE004426.
Moore, H.J., Jakosky, B.M., 1989. Viking landing sites, remote-sensing observations, and physical properties of martian surface materials. Icarus 81, 164–184. https://doi.org/10.1016/0019-1035(89)90132-2.
Moore, H.J., Bickler, D.B., Crisp, J.A., Eisen, H.J., Gensler, J.A., Haldemann, A.F.C., Matijevic, J.R., Reid, L.K., Pavlics, F., 1999. Soil-like deposits observed by Sojourner, the Pathfinder rover. J. Geophys. Res. 104, 8729–8746. https://doi.org/10.1029/1998JE900005.
Morris, R.V., Golden, D.C., Bell III, J.F., Lauer Jr., H.V., Adams, J.B., 1993. Pigmenting agents in martian soils: inferences from spectral Mössbauer, and magnetic properties of nanophase and other iron oxides in Hawaiian palagonitic soil PN-9. Geochim. Cosmochim. Acta 57, 4597–4609. https://doi.org/10.1016/0016-7037(93)90185-Y.
Morris, R.V., Golden, D.C., Ming, D.W., Shelfer, T.D., Jørgensen, L.C., Bell III, J.F., Grafff, T.G., Mertzman, S.A., 2001. Phyllosilicate-poor palagonitic dust from Mauna Kea Volcano (Hawaii): a mineralogical analogue for magnetic Martian dust? J. Geophys. Res. 106, 5057–5083. https://doi.org/10.1029/2000JE001328.
Morris, R.V., Ming, D.W., Gellert, R., Vaniman, D.T., Bish, D.L., Blake, D.F., Chipera, S.J., Morrison, S.M., Downs, R.T., Rampe, E.B., Treiman, A.H., Yen, A.S., Achilles, C.N., Archer Jr., P.D., Bristow, T.F., Cavanagh, P., Fendrich, K., Crisp, J.A., Des Marais, D.J., Farmer, J.D., Grotzinger, J.P., Mahaffy, P.R., McAdam, A.C., Morookian, J.M., MSL Science Team, 2015. Update on the chemical composition of crystalline, smectite, and amorphous components for rocknest soil and john klein and cumberland mudstone drill fines at Gale Crater, Mars. In: Proceedings of the 46th Lunar and Planetary Science Conference, XLVI, 46 Abstract #2622.
Murchie, S.L., Mustard, J., Ehlmann, B.L., Milliken, R.E., Bishop, J.L., McKeown, N.K., Noe Dobrea, E.Z., Seelos, F.P., Buczkowski, D.L., Wiseman, S.M., Arvidson, R.E., Wray, J.J., Swayze, G., Clark, R.N., Des Marais, D.J., McEwen, A.S., Bibring, J.-P., 2009. A synthesis of Martian aqueous mineralogy after 1 Mars year of observations from the Mars Reconnaissance Orbiter. J. Geophys. Res. 114, E00D06. https://doi.org/10.1029/2009JE003342.
Nørnberg, P., Gunnlaugsson, H.P., Merrison, J.P., Vendelboe, A.L., 2009. Salten Skov 1: a Martian magnetic dust analogue. Planet. Space Sci. 57, 628–631. https://doi.org/10.1016/j.pss.2008.08.017.
Osterloo, M.M., Hamilton, V.E., Bandfield, J.L., Glotch, T.D., Baldridge, A.M., Christensen, P.R., Tornabene, L.L., Anderson, F.S., 2008. Chloride-bearing materials in the southern highlands of Mars. Science 319, 1651–1654. https://doi.org/10.1126/science.1150690.
Peters, G.H., Abbey, W., Bearman, G.H., Mungas, G.S., Smith, J.A., Anderson, R.C., Douglas, S., Beegle, L.W., 2008. Mojave Mars simulant – characterization of a new geologic Mars analog. Icarus 197, 470–479. https://doi.org/10.1016/j.icarus.2008.05.004.
Pike, W.T., Staufer, U., Hecht, M.H., Goetz, W., Parrat, D., Sykulska-Lawrence, H., Vijendran, S., Madsen, M.B., 2011. Quantification of the dry history of the Martian soil inferred from in situ microscopy. Geophys. Res. Lett. 38, L24201. https://doi.org/10.1029/2011GL049896.
Poulet, F., Bibring, J.-P., Mustard, J.F., Gendrin, A., Mangold, N., Langevin, Y., Arvidson, R.E., Gondet, B., Gomez, C., 2005. Phyllosilicates on Mars and implications for early martian climate. Nature 438, 623–627. https://doi.org/10.1038/nature04274.
Rampe, E.B., Morris, R.V., Archer Jr., P.D., Agresti, D.G., Ming, D.W., 2016. Recognizing sulfate and phosphate complexes chemisorbed onto nanophase weathering products on Mars using in-situ and remote observations. Am. Mineral. 101, 678–689. https://doi.org/10.2138/am-2016-5408CCBYNCND.
Schrader, C.M., Rickman, D.L., McLemore, C.A., Fikes, J.C., 2010. Lunar Regolith Simulant User's Guide. NASA Marshall Space Flight Center, Ala NASA Technical Memorandum 2010–216446.
Schuerger, A.C., Golden, D.C., Ming, D.W., 2012. Biotoxicity of Mars soils: 1. Dry deposition of analog soils on microbial colonies and survival under Martian conditions. Planet. Space Sci. 72, 91–101. https://doi.org/10.1016/j.pss.2012.07.026.
Scott, A.N., Oze, C., Tang, Y., O'Loughlin, A., 2017. Development of a Martian regolith simulant for in-situ resource utilization testing. Acta Astron. 131, 45–49. https://doi.org/10.1016/j.actaastro.2016.11.024.
Shkuratov, Y., Ovcharenko, A., Zubko, E., Miloslavskaya, O., Muinonen, K., Piironen, J., Nelson, R., Smythe, W., Rosenbush, V., Helfenstein, P., 2002. The opposition effect and negative polarization of structural analogs for planetary regoliths. Icarus 159, 396–416. https://doi.org/10.1006/icar.2002.6923.
Sklute, E.C., Jensen, H.B., Rogers, A.D., Reeder, R.J., 2015. Morphological, structural, and spectral characteristics of amorphous iron sulfates. J. Geophys. Res. 120, 809–830. https://doi.org/10.1002/2014JE004784.
Smith, P.H., Tamppari, L.K., Arvidson, R.E., Bass, D., Blaney, D., Boynton, W.V., Carswell, A., Catling, D.C., Clark, B.C., Duck, T., DeJong, E., Fisher, D., Goetz, W., Gunnlaugsson, H.P., Hecht, M.H., Hipkin, V., Hoffman, J., Hviid, S.F., Keller, H.U., Kounaves, S.P., Lange, C.F., Lemmon, M.T., Madsen, M.B., Markiewicz, W.J., Marshall, J., McKay, C.P., Mellon, M.T., Ming, D.W., Morris, R.V., Pike, W.T., Renno, N., Staufer, U., Stoker, C., Taylor, P., Whiteway, J.A., Zent, A.P., 2009. H_2O at the phoenix landing site. Science 325, 58–61. https://doi.org/10.1126/science.1172339.
Squyres, S.W., Arvidson, R.E., Ruff, S., Gellert, R., Morris, R.V., Ming, D.W., Crumpler, L., Farmer, J.D., Des Marais, D.J., Yen, A., McLennan, S.M., Calvin, W., Bell III, J.F., Clark, B.C., Wang, A., McCoy, T.J., Schmidt, M.E., de Souza Jr., P.A., 2008. Detection of silica-rich deposits on Mars. Science 320, 1063–1067. https://doi.org/10.1126/science.1155429.
Stern, J.C., Sutter, B., Freissinet, C., Navarro-González, R., McKay, C.P., Archer Jr., P.D., Buch, A., Brunner, A.E., Coll, P., Eigenbrode, J.L., Fairen, A.G., Franz, H.B., Glavin, D.P., Kashyap, S., McAdam, A.C., Ming, D.W., Steele, A., Szopa, C., Wray, J.J., Martín-Torres, F.J., Zorzano, M.-P., Conrad, P.M., Mahaffy, P.R., MSL Science Team, 2015. Evidence for indigenous nitrogen in sedimentary and aeolian deposits from the curiosity rover investigations at Gale Crater, Mars. PNAS 112, 4245–4250. https://doi.org/10.1073/pnas.1420932112.
Stroncik, N.A., Schmincke, H.-U., 2002. Palagonite – a review. Int. J. Earth Sci. 91, 680–697. https://doi.org/10.1007/s00531-001-0238-7.
Sutter, B., McAdam, A.C., Mahaffy, P.R., Ming, D.W., Edgett, K.S., Rampe, E.B., Eigenbrode, J.L., Franz, H.B., Freissinet, C., Grotzinger, J.P., Steele, A., House, C.H., Archer Jr., P.D., Malespin, C.A., Navarro-González, R., Stern, J.C., Bell III, J.F., Calef, F.J., Gellert, R., Glavin, D.P., Thompson, L.M., Yen, A.S., 2017. Evolved gas analyses of sedimentary rocks and eolian sediment in Gale Crater, Mars: results of the curiosity rover's sample analysis at Mars (SAM) instrument from Yellowknife Bay to the Namib Dune. J. Geophys. Res. 122, 2564–2609. https://doi.org/10.1002/2016JE005225.
Taylor, S.R., McLennan, S.M, 2009. Planetary Crusts: Their Composition, Origin and Evolution. Cambridge University Press.
Taylor, L.A., Pieters, C.M., Britt, D., 2016. Evaluations of lunar regolith simulants. Planet. Space Sci. 126, 1–7. https://doi.org/10.1016/j.pss.2016.04.005.
Toon, O.B., Pollack, J.B., Sagan, C., 1977. Physical properties of the particles composing the Martian dust storm of 1971-1972. Icarus 30, 663–696. https://doi.org/10.1016/0019-1035(77)90088-4.
Wamelink, G.W.W., Frissel, J.Y., Krijnen, W.H.J., Verwoert, M.R., Goedhart, P.W., 2014. Can plants grow on Mars and the Moon: a growth experiment on Mars and Moon soil simulants. PLoS One 9, e103138. https://doi.org/10.1371/journal.pone.0103138.
Wellington, D.F., Bell III, J.F., Johnson, J.F., Kinch, K.M., Rice, M.R., Godber, A., Ehlmann, B.L., Fraeman, A.A., Hardgrove, C., MSL Science Team, 2017. Visible to near-infrared MSL/Mastcam multispectral imaging: initial results from select high-interest science targets within Gale Crater, Mars. Am. Mineral. 102, 1202–1217. https://doi.org/10.2138/am-2017-5760CCBY.
Yen, A.S., Gellert, R., Schröder, C., Morris, R.V., Bell III, J.F., Knudson, A.T., Clark, B.C., Ming, D.W., Crisp, J.A., Arvidson, R.E., Blaney, D., Brückner, J., Christensen, P.R., DesMarais, D.J., de Souza Jr., P.A., Economou, T.E., Ghosh, A., Hahn, B.C., Herkenhoff, K.E., Haskin, L.A., Hurowitz, J.A., Joliff, B.L., Johnson, J.R., Klingelhöfer, G., Maden, M.B., McLennan, S.M., McSween, H.Y., Richter, L., Rieder, R., Rodinov, D., Soderblom, L., Squyres, S.W., Tosca, N.J., Wang, A., Wyatt, M., Zipfel, J., 2005. An integrated view of the chemistry and mineralogy of martian soils. Nature 436, 49–54. https://doi.org/10.1038/nature03637.
Yen, A.S., Gellert, R., Clark, B.C., Ming, D.W., King, P.L., Schmidt, M.E., Leshin, L., Morris, R.V., Squyres, S.W., Spray, J., Campbell, J.L., MSL Science Team, 2013. Evidence for a global martian soil composition extends to Gale Crater. In: Proceedings opf the Lunar and Planetary Science Conference, XLIV, 44 Abstract #2495.
Zacny, K., Paulsen, G., McKay, C.P., Glass, B., Davé, A., Davila, A.F., Marinova, M., Mellerowicz, B., Heldmann, J., Stoker, C., Cabrol, N., Hedlund, M., Craft, J., 2013. Reaching 1m deep on Mars: the icebreaker drill. Astrobiology 13, 1166–1198. https://doi.org/10.1089/ast.2013.1038.
Zeng, X., Li, X., Wang, S., Li, S., Spring, S., Tang, H., Li, Y., Feng, J., 2015. JMSS-1: a new Martian soil simulant. Earth Planets Space 67. https://doi.org/10.1186/s40623-015-0248-5.